

Rough Surface Scattering Analysis at 60 GHz in an Underground Mine Gallery

Shah Ahsanuzzaman Md Tariq*, Charles Despins†, Sofiène Affes‡ and Chahé Nerguizian*

*Université de Montréal-École Polytechnique, Montreal, Canada

†PROMPT-Quebec, Montreal, Canada

‡INRS-EMT, Université du Québec, Montreal, Canada

Corresponding emails: tariq.shah-ahsanuzzaman-md@polymtl.ca, CDDespins@promptinc.org,
affes@emt.inrs.ca, chahe.nerguizian@polymtl.ca

Abstract—60 GHz wireless communication systems are promising wireless gigabit transmission supports for short-range multimedia communications, particularly in niche applications such as in underground mines. In order to investigate the behavior of an underground mine channel with a 5 mm wavelength and with centimetre range surface roughness of the mine walls, signal scattering characteristics have been investigated. In this paper, the statistical distribution of surface parameters such as heights and correlation coefficients are extracted from the measurements, in order to quantify the roughness of mine walls. Kirchhoff approximation (KA) scattering has been used to characterize one single Radar Cross Section scattering behavior. The angular dependent received power has been examined from both simulations and measurements. As such, this paper develops a KA model, for 60 GHz underground mine communications, which is validated by experimental results.

Index Terms—Kirchhoff scattering, surface height distribution, 60 GHz propagation measurements.

I. INTRODUCTION

Recently, the use of WLANs is facing increasing demand from multimedia communications and creating new research challenges for operation in home or commercial environments. The millimeter (mm) wave band from 20 to 60 GHz is seen by many researchers as a possible solution for wireless broadband communication systems [1]. For example, in cellular and peer to peer angle dependent wireless propagation at 60 GHz, study provides the importance of scattering from foliage/vegetation, tree trunks and bricks, and the result shows that the single bounce scattering produces more links than double bounce scattering [2]. However, in niche markets such as underground mines, automation and security requirements are driving to the development of 60 GHz wireless communication systems. With a 5 mm wavelength, the scattering phenomena due to the high roughness of the mine surface may cause a non-negligible multipath contribution at each respective antenna element and hence have to be taken into account. Various standard theoretical scattering models are described in the open literature such as Kirchhoff Models which consists of the Geometrical Optics Model, Physical Optics Model based on ray optics to estimate the electric field on a surface and the Small Perturbation Model which is dominated by the coherent component of scattering [3]. The scattering patterns for a Kirchhoff model surface are

dominated by the diffuse components. The small perturbation approximation requires small standard deviation of heights and correlation lengths with respects to the wavelength. Therefore, based on the explanation and validation of models, Kirchhoff scattering models are suitable for high rough surfaces whereas a Physical Optics Model is mostly considered for average roughness and small perturbation approximation is well suited for small roughness. A suitable analytical approach of Kirchhoff scattering approximation commonly found in literature, is widely used for scattering analysis [4]. Non specular, specular and diffused scattering analysis and measurement at THz frequency are cited in [5]–[8]. The multiplication of the reflection coefficient, derived from the Fresnel equations, with the Rayleigh roughness factor is considered as the extension of the Kirchhoff theory of scattering [4]. This theory is thoroughly implemented in THz communication for home environments [5]. Also, backscattering measurement procedures and measured reflected signal from strong reflections by buildings in urban areas have been analyzed at a 4 GHz frequency and have been found to be 20 to 30 dB higher than diffused scattered energy [9].

The scattering phenomena in underground mine environments, can be solved by KA theory and its ray tracing simulation tool may be used in order to obtain the power delay profile of the channel. The Kirchhoff approximation (KA) has to be employed to find a model of the channel. Measurements are necessary for the model verification. In order to validate KA in an underground mine, surface height measurements have been carried out. After extracting the roughness parameters, channel measurements at 60 GHz have been performed and validated with the model.

This paper is structured as follows: in Section II, the Kirchhoff scattering approach is introduced. Surface roughness measurements as well as calculation of the roughness parameters are exposed in section III. Section IV presents 60 GHz wideband channel scattering measurement setup and procedure. The implementation of KA model based on surface parameters is presented and matched with measurement results in section V. Finally conclusions are given in Section VI.

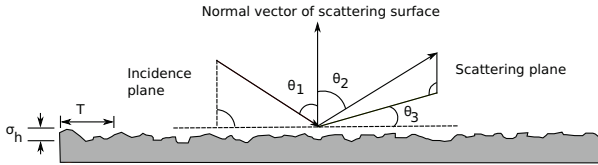


Fig. 1: Rough surface scattering geometry.

II. KIRCHHOFF SCATTERING APPROXIMATION

Beckmann and Spizzichino derive an analytical description of the electromagnetic field scattered from a rough surface [4]. A schematic illustration of the corresponding geometry is given in Fig 1, where θ_1 is the incident angle, θ_2 is the azimuth angle referred as reflection angle and θ_3 is the elevation angle of the scattered signal. Scattered field over the entire surface needs to be considered in order to obtain the scattering coefficient ρ with the assumption of a Gaussian height distribution. Such surface is characterized by its heights standard deviation σ_h and its surface correlation length T . Knowing the angles θ_1 , θ_2 and θ_3 , the average scattering coefficient for an infinite surface is given, for a roughness factor g equal to 1 or less than 1, by

$$\langle \rho \rho^* \rangle_\infty = e^{-g} \cdot \left(\rho_0^2 + \frac{\pi T^2 F^2}{A} \sum_{m=1} \frac{g^m}{m! m!} e^{-\frac{v_{xy}^2 T^2}{4m}} \right) \quad (1)$$

where ρ_0^2 describes the scattering in specular direction and the second term of (1) is defined as the diffuse scattering. The Rayleigh roughness factor g is an indicator for the relative surface roughness at a given wavelength. Other parameters of this equation are given below

$$\rho_0 = \text{sinc}(v_x l_x) \cdot \text{sinc}(v_y l_y), \quad (2)$$

$$v_x = k \cdot (\sin(\theta_1) - \sin(\theta_2) \cos(\theta_3)), \quad (3)$$

$$v_y = k \cdot (-\sin(\theta_2) \sin(\theta_3)), \quad (4)$$

$$v_{xy} = \sqrt{v_x^2 + v_y^2}, \quad (5)$$

$$v_z = 2k \cos(\theta_1), \quad (6)$$

$$F = \frac{1 + \cos(\theta_1) \cos(\theta_2) - \sin(\theta_1) \sin(\theta_2) \cos(\theta_3)}{\cos(\theta_1)(\cos(\theta_1) + \cos(\theta_2))}, \quad (7)$$

$$g = k^2 \sigma_h^2 (\cos(\theta_1) + \cos(\theta_2))^2 \quad (8)$$

Where $k = 2\pi/\lambda$ is the wave number and $A = l_x \cdot l_y$ is the surface area. The value of l_x and l_y of the scattering surface has to be chosen large compared to the wavelength (λ) and the correlation length (T). When $g \gg 1$, the special case of KA scattering becomes:

$$\langle \rho \rho^* \rangle_\infty = \frac{\pi T^2 F^2}{A v_z^2 \sigma_h^2} e^{-\frac{v_{xy}^2 T^2}{4 v_z^2 \sigma_h^2}} \quad (9)$$

It has to be noted that the value of σ_h , T and λ are related to each other through (8) and (9). If σ_h is low and T is high,



Fig. 2: Wall surface height measurement at 40 m mine gallery.

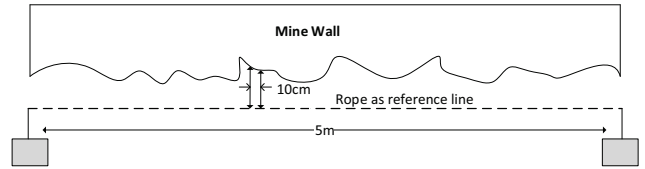


Fig. 3: Height measurement procedure.

then the value of g will be less than or equal to 1 which tends to a smooth surface creating specular reflections.

III. SURFACE HEIGHT CHARACTERISTICS

In order to extract the surface parameters from the mine wall, a 40 m underground level CANMET gold mine gallery (in Val d'Or) has been considered as shown in Fig. 2. The width and height of the gallery are approximately 5 m.

A. Height measurement

A mine wall area of $1.5m \times 5m$ has been used to measure manually the surface roughness height with a grid spacing of 10 cm by using a fixed rope. The measurement procedure is shown in Fig. 3. The 10 cm grid spacing is taken as an initial guess for surface height measurement. Even though the horizontal and vertical resolution of height measurement is 10 cm, the surface heights have been assumed to be symmetric in the whole gallery of 40 m level depth. Moreover, it has been also observed that the roughness of the walls, ceiling and floor have different characteristics in nature.

B. Roughness Characterization

1) *Height distribution:* The surface height distribution describes the two dimensional variation in surface elevation and azimuth above an arbitrary plane. A higher resolution will provide more accurate surface roughness, which is defined by the standard deviation of the surface heights' distribution. This parameter has a paramount importance in statistical methods

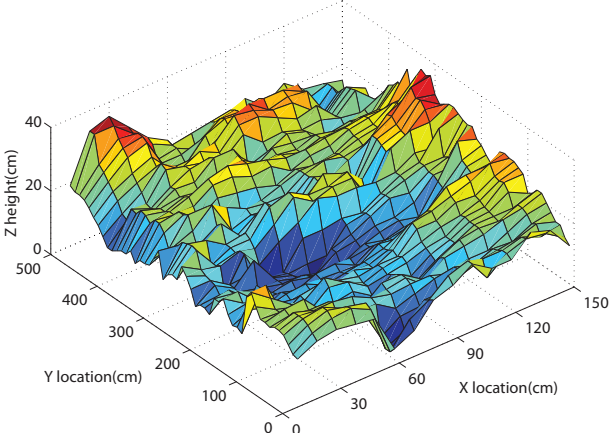


Fig. 4: 3D color map of measured surface height distribution.

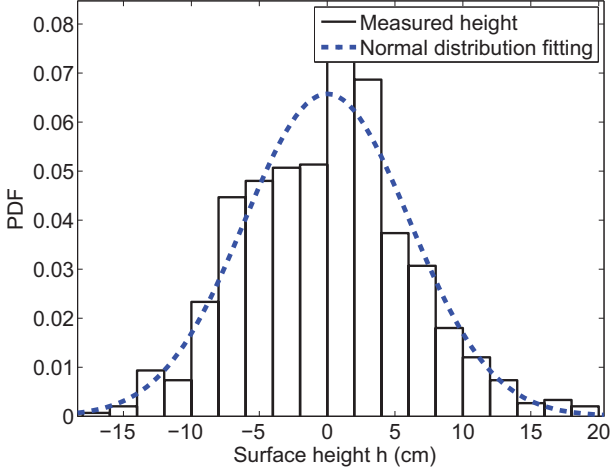
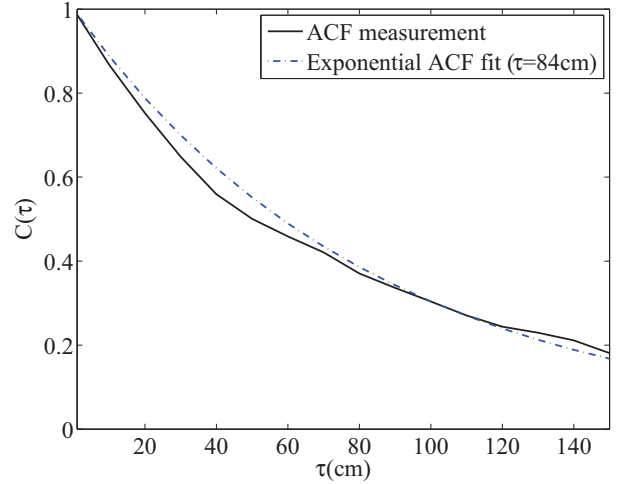


Fig. 5: Probability distribution of measured surface heights.

for roughness calculation purposes. It is more sensitive than the arithmetic average of heights. The surface height distribution of the measured area is obtained by processing the measured surface roughness data using $h_{x,y} = h_{x,y_{max}} - h_{x,y_{ref}}$, where x, y are the grid index, $h_{x,y}$ is the roughness heights of the wall, $h_{x,y_{ref}}$ is the value of heights to the reference line and $h_{x,y_{max}}$ is the maximum value between the reference line and the rough point. Fig. 4 shows the color map of the spatial distribution of the wall surface. Maximum and average heights are found to be 37.5 cm and 20.5 cm, respectively. The measured heights were then fitted with a normal distribution in order to find statistical parameters as shown in Fig. 5. It can be seen that, the wall surface has a Gaussian distribution with zero mean and 6.0658 cm of standard deviation (σ_h).

2) Height correlation: The correlation length describes how strongly the surface heights of neighbouring points are correlated. In other terms, the correlation length provides information whether the surface consists of densely packed irregularities or slowly varying features. It can be defined

Fig. 6: Auto correlation function of the heights $C(\tau)$.

as the distance between two statistically independent points. Generally, the autocorrelation decreases when the distance increases and is determined empirically using the auto correlation function (ACF) which is equal to $C(\tau) = \langle h_1 h_2 \rangle / \langle h_1^2 \rangle$, where h_1 and h_2 are two heights and τ is the distance between them. For instance, the discrete one-dimensional auto correlation function $C(\tau)$ can be determined from two dimensional ($N \times M$) discrete heights $h_{x,y}$ and is given by,

$$C(\tau) = \sum_{\tau=1}^N \sum_{x=1}^N \left[\frac{\sum_{y=1}^{M-\tau} h_{x,y} h_{x,y+\tau}}{\sum_{y=1}^M h_{x,y}^2} \right] \quad (10)$$

where $x = 1, 2, \dots, N$ and $y = 1, 2, \dots, M$. The correlation length is then defined as the value of τ at which the autocorrelation coefficient $C(\tau)$ drops to e^{-1} . According to exponential fitting as shown in Fig. 6, the correlation length T is found to be 84 cm.

The channel measurements have been carried out at the 70 m level of mine. However, due to time constraint, surface height measurements have been done only at the 40 m level of the mine gallery. Hence, in this paper it has been assumed that the height distribution at 70 m level is similar to the one at 40 m.

IV. SCATTERING MEASUREMENT

A. Scattered power measurement setup and procedure

As reference, there are some back scattering measurement techniques illustrated in the literature [10], [11]. In order to find backscattered power from the wall, a 60 GHz wideband measurement system setup has been used in the underground mine environment. A measurement campaign in static condition, has been carried out at 70 m level in the CANMET mine located in Val d'Or, Quebec as shown in Fig 7. The measurement setup is based on 60 GHz cable architecture. A Vector Network Analyzer (ANRITSU MS 4647A) with a



Fig. 7: Digital photograph for scattering measurement at 70 m mine gallery.

frequency band range of 40 MHz to 70 GHz has been used. Gain of 30 dB for the Power Amplifier (CBM 57653/015-03 CERNEX) and the Low Noise Amplifier (CBL 57653/055-01 CERNEX) have been used. Additional Low Noise Amplifier (QuinStar, Serial N11328, Model 001001) has been employed, with a gain of 18 dB, to enhance the signal. The frequency range has been selected using the IEEE Standard 802.15.3c which considers a central frequency between 57.24 GHz to 59.4 GHz for a channel 1 high bandwidth model. Other channel models have not been considered in the measurement campaign due to the upper limit range of the QuinStar LNA ($f_c \leq 61$ GHz) and the cable losses. The transmit power was set at 4 dBm. In order to have accurate and fixed position for the transmitter and the scattered points, a pointing laser with a camera tripod have been used. Transmitter and receiver heights were around 1.5 m corresponding to the middle position of the gallery dimension. The data acquisition was completed by connecting a computer to the VNA via a GPIB interface. A Labview program was employed to control the whole measurement procedure and a MATLAB program was applied to rotate the antenna using Velmex 3D table with a step of 5°. A bandwidth of 2.16 GHz has been used with a 1.08 MHz sweep frequency. For the setup configurations, the system noise floor was -107 dB. The system calibration was done with 2000 sweep points for the whole bandwidth of 2.16 GHz with a spacing of 1.08 MHz.

The purpose of the measurement was to validate the KA mode described in the section II and to develop a framework for the application of a ray tracing model suitable for the underground mine. The measurements were part of an experimental program in the CANMET mine mainly focused on the scattering measurements from the wall surface at 70 m level gallery. Figs. 7 and 8 show the experimental arrangement used to measure the scattered signal from the wall. In order to make a far field region of the horn antennas, Tx and Rx were set at 1 m away from the wall with a separation distance

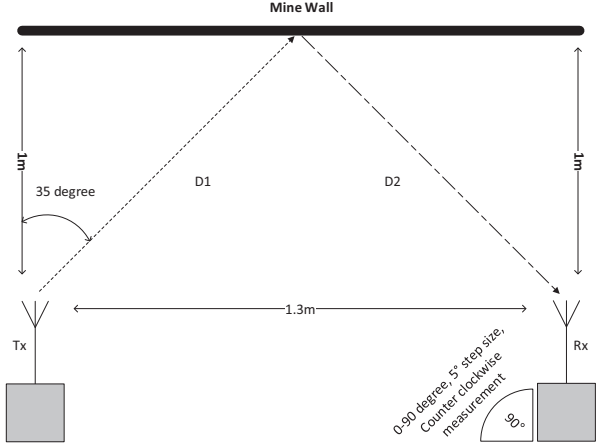


Fig. 8: Illustration of measurement procedure.

of 3 m. Tx was fixed with 35° incident angle and Rx was moved from 3 m to 1 m towards the Tx until a detectable received signal was obtained corresponding to a separation distance of 1.3 m. According to measurement observations, for a Tx-Rx separation distance larger than 3 m, no signal were obtained. As in Fig. 8, $D_1 + D_2$ was calculated from the geometry of the illustration and was found to be 2.23 m. An azimuth incident angle of 35° was set at the transmitter and the receiver was rotated from 0 to 90° along the counter clockwise direction. The rotation was used to see angular dependency of the scattered power from the wall.

V. IMPLEMENTATION AND DISCUSSION

Fig. 9 shows the model of wall scattering which consists of a one radar cross section (RCS) for one single ray. RCS is defined as two times of the correlation length T . A free space propagation from the transmitter to the scattering point and from the scattering point to the receiver has been considered. According to the values of T and σ_h obtained from surface height measurements, and with $\theta_1 = 35^\circ$, the min and max values of roughness factor g are found to be $3.8514e^3$ and $1.8813e^4$, respectively which are much more greater than 1. For this condition, the scattering coefficient for infinite surface $\langle \rho\rho^* \rangle_\infty$ has been considered since it corresponds to the special case ($g \gg 1$) of (9). It has also been observed that T and σ_h of the surface roughness are the main parameters for the simulation process. Simulation results show that increasing the correlation length with a fixed roughness value, gives a less scattering behaviour at the receiver end. Moreover, the incident energy of the signal is scattered more strongly if σ_h increases with a given correlation length. The finite scattering coefficient $\langle \rho\rho^* \rangle_{TE/TM}$, after multiplication of the conventional Fresnel reflection coefficient $r_{TE/TM}$ at 35° incident angle, is determined as

$$\langle \rho\rho^* \rangle_{TE/TM} = (r_{TE/TM} \cdot r_{TE/TM}^*) \cdot \langle \rho\rho^* \rangle_\infty \quad (11)$$

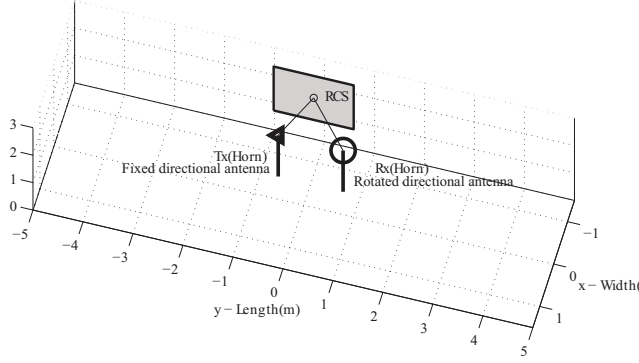


Fig. 9: 3D kirchhoff scattering model for mine.

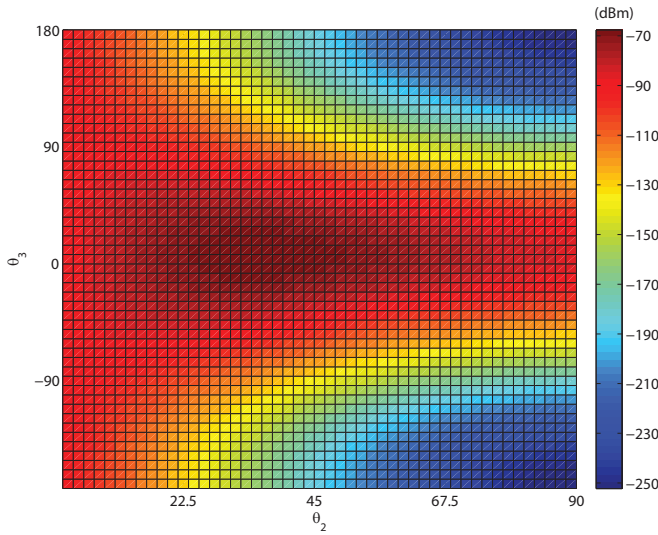
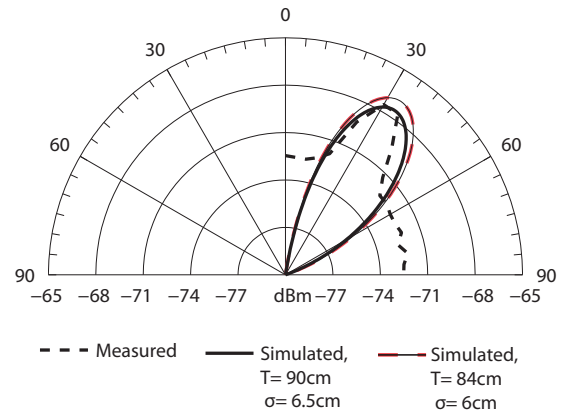


Fig. 10: Simulated angular dependent scattered power.

The received power is then calculated within a given area of $A (l_x \times l_y)$ by multiplying the finite scattering coefficient of Friis formula. It can be calculated as [4], [10]

$$P_r = P_t G_t G_r \left(\frac{\lambda}{4\pi(D1 + D2)} \right)^2 \cdot \langle \rho \rho^* \rangle_{TE/TM} \quad (12)$$

The angular dependent scattered received power corresponding to θ_1 and θ_2 is shown in Fig. 10. It can be noted that, the scattered power is mostly in specular direction θ_2 and it is spread with a broad angular range in θ_3 direction. According to measurement results, pathloss has been calculated from equation 13, where N is the value of the sweep points and $H(f)$ is the transfer function of the channel. $H(f)$ has been calculated by averaging 5 snap shots taken from different time instances.

$$PL(dB) = -10 \log_{10} \left[\frac{1}{N} \sum_{i=1}^N |H(f_i)|^2 \right] \quad (13)$$

Fig. 11: Measured and simulated scattered received power.

The received power is then determined as

$$P_r(dBm) = P_t(dBm) - PL(dB) \quad (14)$$

The received signal from measurements were obtained using the distinguishable peaks associated to the scattered power coming from the wall. Angular dependencies for both measurement and simulation are considered for azimuth angle θ_2 direction. KA Simulation parameter profiles are defined as $[T, \sigma, \theta]$. In this paper, two simulation profile have been used, $[T = 84, \sigma = 6, \theta = 35^\circ]$ and $[T = 90, \sigma = 6.5, \theta = 35^\circ]$ and corresponding plots are shown in Fig. 11. Result of measured received power was found to be approximately equal to the background scattered power from KA model as shown in Fig. 11. It has been shown that simulation parameters $[T, \sigma]$ can be fitted with the measured data which are nearly close to the measured surface characteristic parameters. Only scattered mine walls measurements have been considered (no ceiling and floor) due to time constraint.

The measurements were subsequently repeated for the far-field case, in which the receiver-wall distance was reduced further. Moreover, measurements with cross polarized transmitter and receiver antennas have been performed with no significant reflected signal obtained and the results are not included in this paper. It is clear that a fair agreement between simulated and measured values exists where the scattering power is above -72 dBm. The peak of the scattered power has found to be -68 dBm. It is useful to point out that incident power is scattered significantly around the specular direction (35°) of the reflected signal. The incident power is distributed around the scattering point and the scattered angular range is around 10° . By comparing the maximum scattered power with the line of sight (LOS) measurement, for the same propagation distance of 2.23 m, a 30 dB difference has been found. This LOS measurement was a part of the scattering measurement campaign. Hence, one can conclude that there is an additional

loss of the incident power during scattering from the wall due to surface absorption and roughness of the wall. This scattering phenomena should therefore impact the power delay profile simulations for the entire mine tunnels using the KA model.

VI. CONCLUSION

The study of wall scattering for 60 GHz channel characterization in an underground mine is necessary because incident power is subjected to scattering around the reflected point with 5 mm wavelength and 6 cm wall roughness. This scattering loss is not insignificant for channel characterization in this peculiar environment. The purpose of the analysis was not aimed to arrive to an exact determination of the reflected and scattered power separately but to find out the angular resolution of the scattered power from the wall. In contrast, based on the Kirchhoff Approximation, we have proposed an approach to consider scattering along the specular direction from rough surfaces at 60 GHz. Surface roughness measurements have been analyzed to prove the validity of the model as an intermediate parameter. The measurement results are in fair agreement with the simulation results. It has been shown in the paper that the KA scattering approach could be used to develop a simulation tool for the entire gallery at a 60 GHz frequency in underground mine environments. Further investigations may be carried out to determine the scattering loss coefficients associated with mine floors, walls and ceilings.

REFERENCES

- [1] S. K. Yong, P. Xia, and A. V. Garcia, *60 GHz Technology for Gbps WLAN and WPAN: From Theory to Practice*. Wiley, 2011.
- [2] T. Rappaport, E. Ben-Dor, J. Murdock, and Y. Qiao, "38 GHz and 60 GHz angle-dependent propagation for cellular and peer-to-peer wireless communications," in *Communications (ICC), 2012 IEEE International Conference on*, June 2012, pp. 4568–4573.
- [3] V. Gupta and R. Jangid, "Microwave response of rough surfaces with auto-correlation functions, rms heights and correlation lengths using active remote sensing," *Indian Journal of Radio and Space Physics*, vol. 40, no. 3, pp. 137 – 46, 2011.
- [4] P. Beckmann and A. Spizzichino, *The Scattering of Electromagnetic Waves from Rough Surfaces*, ser. International Series of Monographs on Electromagnetic Waves. Pergamon Press, 1963.
- [5] R. Piesiewicz, C. Jansen, D. Mittleman, T. Kleine-Ostmann, M. Koch, and T. Kurner, "Scattering analysis for the modeling of THz communication systems," *IEEE Transactions on Antennas and Propagation*, vol. 55, no. 11, pp. 3002 – 9, 2007.
- [6] S. Priebe, M. Jacob, C. Jansen, and T. Kurner, "Non-specular scattering modeling for THz propagation simulations," in *Proceedings of the 5th European Conference on Antennas and Propagation, EUCAP 2011*, Rome, Italy, 2011, pp. 1 – 5.
- [7] S. Priebe, M. Jacob, and T. Kurner, "Polarization investigation of rough surface scattering for THz propagation modeling," in *Proceedings of the 5th European Conference on Antennas and Propagation, EUCAP 2011*, Rome, Italy, 2011, pp. 24 – 28.
- [8] C. Jansen, S. Priebe, C. Moller, M. Jacob, H. Dierke, M. Koch, and T. Kurner, "Diffuse scattering from rough surfaces in THz communication channels," *IEEE Transactions on Terahertz Science and Technology*, vol. 1, no. 2, pp. 462 – 72, 2011.
- [9] A. Noerpel, M. Krain, and A. Ranade, "Measured scattered signals at 4 GHz confirm strong specular reflections off buildings," *Electronics Letters*, vol. 27, no. 10, pp. 869 – 71, 1991.
- [10] G. Conway, L. Schott, and A. Hirose, "Measurement of surface reflection coefficients via multiple reflection of microwaves," *Review of Scientific Instruments*, vol. 65, no. 9, pp. 2920 – 2920, 1994.
- [11] M. Al-Nuaimi and M. Ding, "Prediction models and measurements of microwave signals scattered from buildings," *IEEE Transactions on Antennas and Propagation*, vol. 42, no. 8, pp. 1126 – 37, 1994.